

Measurements of the Cross Section for $e^+e^- \rightarrow$ hadrons at Center-of-Mass Energies from 2 to 5 GeV

J. Z. Bai¹, Y. Ban¹⁰, J. G. Bian¹, A. D. Chen¹, H. F. Chen¹⁶, H. S. Chen¹, J. C. Chen¹, X. D. Chen¹, Y. B. Chen¹, B. S. Cheng¹, S. P. Chi¹, Y. P. Chu¹, J. B. Choi³, X. Z. Cui¹, Y. S. Dai¹⁹, L. Y. Dong¹, Z. Z. Du¹, W. Dunwoodie¹⁴, H. Y. Fu¹, L. P. Fu⁷, C. S. Gao¹, S. D. Gu¹, Y. N. Guo¹, Z. J. Guo², S. W. Han¹, Y. Han¹, F. A. Harris¹⁵, J. He¹, J. T. He¹, K. L. He¹, M. He¹¹, X. He¹, T. Hong¹, Y. K. Heng¹, G. Y. Hu¹, H. M. Hu¹, Q. H. Hu¹, T. Hu¹, G. S. Huang², X. P. Huang¹, Y. Z. Huang¹, J. M. Izen¹⁷, X. B. Ji¹¹, C. H. Jiang¹, Y. Jin¹, B. D. Jones¹⁷, J. S. Kang⁸, Z. J. Ke¹, H. J. Kim¹³, S. K. Kim¹³, T. Y. Kim¹³, D. Kong¹⁵, Y. F. Lai¹, D. Li¹, H. B. Li¹, H. H. Li⁶, J. Li¹, J. C. Li¹, P. Q. Li¹, Q. J. Li¹, R. Y. Li¹, W. Li¹, W. G. Li¹, X. N. Li¹, X. Q. Li⁹, B. Liu¹, F. Liu⁶, Feng Liu¹, H. M. Liu¹, J. Liu¹, J. P. Liu¹⁸, T. R. Liu¹, R. G. Liu¹, Y. Liu¹, Z. X. Liu¹, X. C. Lou¹⁷, G. R. Lu⁵, F. Lu¹, J. G. Lu¹, Z. J. Lu¹, X. L. Luo¹, E. C. Ma¹, J. M. Ma¹, R. Malchow⁴, H. S. Mao¹, Z. P. Mao¹, X. C. Meng¹, X. H. Mo¹, J. Nie¹, Z. D. Nie¹, S. L. Olsen¹⁵, D. Paluselli¹⁵, H. Park⁸, N. D. Qi¹, X. R. Qi¹, C. D. Qian¹², J. F. Qiu¹, Y. K. Que¹, G. Rong¹, Y. Y. Shao¹, B. W. Shen¹, D. L. Shen¹, H. Shen¹, X. Y. Shen¹, H. Y. Sheng¹, F. Shi¹, H. Z. Shi¹, X. F. Song¹, J. Y. Suh⁸, H. S. Sun¹, L. F. Sun¹, Y. Z. Sun¹, S. Q. Tang¹, W. Toki⁴, G. L. Tong¹, G. S. Varner¹⁵, J. Wang¹, J. Z. Wang¹, L. Wang¹, L. S. Wang¹, P. Wang¹, P. L. Wang¹, S. M. Wang¹, Y. Y. Wang¹, Z. Y. Wang¹, C. L. Wei¹, N. Wu¹, D. M. Xi¹, X. M. Xia¹, X. X. Xie¹, G. F. Xu¹, Y. Xu¹, S. T. Xue¹, W. B. Yan¹, W. G. Yan¹, C. M. Yang¹, C. Y. Yang¹, G. A. Yang¹, H. X. Yang¹, W. Yang⁴, X. F. Yang¹, M. H. Ye², S. W. Ye¹⁶, Y. X. Ye¹⁶, C. S. Yu¹, C. X. Yu¹, G. W. Yu¹, Y. Yuan¹, B. Y. Zhang¹, C. Zhang¹, C. C. Zhang¹, D. H. Zhang¹, H. L. Zhang¹, H. Y. Zhang¹, J. Zhang¹, J. W. Zhang¹, L. Zhang¹, L. S. Zhang¹, P. Zhang¹, Q. J. Zhang¹, S. Q. Zhang¹, X. Y. Zhang¹¹, Y. Y. Zhang¹, Z. P. Zhang¹⁶, D. X. Zhao¹, H. W. Zhao¹, Jiawei Zhao¹⁶, J. W. Zhao¹, M. Zhao¹, P. P. Zhao¹, W. R. Zhao¹, Y. B. Zhao¹, Z. G. Zhao¹, J. P. Zheng¹, L. S. Zheng¹, Z. P. Zheng¹, B. Q. Zhou¹, G. M. Zhou¹, L. Zhou¹, K. J. Zhu¹, Q. M. Zhu¹, Y. C. Zhu¹, Y. S. Zhu¹, Z. A. Zhu¹, B. A. Zhuang¹, and B. S. Zou¹.

(BES Collaboration)

¹ Institute of High Energy Physics, Beijing 100039, People's Republic of China

² China Center of Advanced Science and Technology, Beijing 100080, People's Republic of China

³ Chonbuk National University, Chonju 561-756, Korea

⁴ Colorado State University, Fort Collins, Colorado 80523

⁵ Henan Normal University, Xinxiang 453002, People's Republic of China

⁶ Huazhong Normal University, Wuhan 430079, People's Republic of China

⁷ Hunan University, Changsha 410082, People's Republic of China

⁸ Korea University, Seoul 136-701, Korea

⁹ Nankai University, Tianjin 300071, People's Republic of China

¹⁰ Peking University, Beijing 100871, People's Republic of China

¹¹ Shandong University, Jinan 250100, People's Republic of China

¹² Shanghai Jiaotong University, Shanghai 200030, People's Republic of China

¹³ Seoul National University, Seoul 151-742, Korea

¹⁴ Stanford Linear Accelerator Center, Stanford, California 94309

¹⁵ University of Hawaii, Honolulu, Hawaii 96822

¹⁶ University of Science and Technology of China, Hefei 230026, People's Republic of China

¹⁷ University of Texas at Dallas, Richardson, Texas 75083-0688

¹⁸ Wuhan University, Wuhan 430072, People's Republic of China

¹⁹ Zhejiang University, Hangzhou 310028, People's Republic of China

(September 26, 2019)

We report values of $R = \sigma(e^+e^- \rightarrow \text{hadrons})/\sigma(e^+e^- \rightarrow \mu^+\mu^-)$ for 85 center-of-mass energies between 2 and 5 GeV measured with the upgraded Beijing Spectrometer at the Beijing Electron-Positron Collider.

In precision tests of the Standard Model (SM) [1], the quantities $\alpha(M_Z^2)$, the QED running coupling constant evaluated at the Z pole, and $a_\mu = (g-2)/2$, the anomalous magnetic moment of the muon, are of fundamental importance. The dominant uncertainties in both $\alpha(M_Z^2)$ and a_μ^{SM} are due to the effects of hadronic vacuum polarization, which cannot be reliably calculated in the low energy region. Instead, with the application of dispersion relations, experimentally measured R values are used to determine the vacuum polarization, where R is the lowest order cross section for $e^+e^- \rightarrow \gamma^* \rightarrow \text{hadrons}$ in units of the lowest-order QED cross section for $e^+e^- \rightarrow \mu^+\mu^-$, namely $R = \sigma(e^+e^- \rightarrow \text{hadrons})/\sigma(e^+e^- \rightarrow \mu^+\mu^-)$, where $\sigma(e^+e^- \rightarrow \mu^+\mu^-) = \sigma_{\mu\mu}^0 = 4\pi\alpha^2(0)/3s$.

Values of R in the center-of-mass (cm) energy range below 5 GeV were measured about 20 years ago with a precision of 15 – 20% [2–4]. In this paper, we report measurements of R at 85 cm energies between 2 and 4.8 GeV, with an average precision of 6.6% [5]. Results from a preliminary scan that measured R at 6 energy points between 2.6 and 5 GeV have been reported previously [6].

The measurements were carried out with the upgraded Beijing Spectrometer (BESII) at the Beijing Electron-Positron Collider (BEPC). BESII is a conventional collider detector based on a large solenoid magnet with a central field of 0.4 T and is described in detail in ref. [7]. In order to understand beam-associated backgrounds, separated beam data were accumulated at 24 different energies interspersed throughout the entire energy range. Special runs were taken at the J/ψ and $\psi(2S)$ resonances were scanned at the beginning and end of the R scan to calibrate the cm energy, E_{cm} .

Experimentally, the value of R is determined from the number of observed hadronic events, N_{had}^{obs} , by the relation

$$R = \frac{N_{had}^{obs} - N_{bg} - \sum_l N_{ll} - N_{\gamma\gamma}}{\sigma_{\mu\mu}^0 \cdot L \cdot \epsilon_{had} \cdot \epsilon_{trg} \cdot (1 + \delta)}, \quad (1)$$

where N_{bg} is the number of beam-associated background events; $\sum_l N_{ll}$, ($l = e, \mu, \tau$) are the numbers of lepton-pair events from one-photon processes and $N_{\gamma\gamma}$ the number of two-photon process events that are misidentified as hadronic events; L is the integrated luminosity; δ is the effective initial state radiative (ISR) correction; ϵ_{had} is the detection efficiency for hadronic events; and ϵ_{trg} is the trigger efficiency.

The triggers and the determination of the trigger efficiency were the same as those used in our previous R

scan [6]. The trigger efficiencies, measured by comparing the responses to different trigger requirements in the R scan data, as well as in special runs taken at the J/ψ resonance, are determined to be 99.96%, 99.33% and 99.76% for Bhabha, dimuon and hadronic events, respectively. The errors are 0.5%.

We use a set of requirements on fiducial regions, vertex positions, track fit quality, maximum and minimum Barrel Shower Counter (BSC) energy deposition, track momenta and time-of-flight hits to preferentially distinguish one-photon multi-hadron production from all possible contamination mechanisms. After the imposition of these requirements, the remaining backgrounds are due to cosmic rays, lepton pair production, two-photon interactions and single-beam-related processes. Additional requirements are imposed on two-prong events, for which cosmic ray and lepton pair backgrounds are especially severe.

An acceptable charged track must be in the polar angle region $|\cos\theta| < 0.84$, have a good helix fit, and not be clearly identified as an electron or muon. The distance of closest approach to the beam axis must be less than 2 cm in the transverse plane, and must occur at a point along the beam axis for which $|z| < 18$ cm. In addition, the following criteria must be satisfied: (i) $p < p_{beam} + 5 \times \sigma_p$, where p and p_{beam} are the track and incident beam momenta, respectively, and σ_p is the momentum uncertainty for a charged track for which $p = p_{beam}$; (ii) $E < 0.6E_{beam}$, where E is the BSC energy associated with the track, and E_{beam} is the beam energy; (iii) $2 < t < t_p + 5 \times \sigma_t$ (in ns.), where t is the measured time-of-flight for the track, t_p is the time-of-flight calculated assigning the proton mass to the track, and σ_t is the resolution of the barrel time-of-flight system.

After track selection, an event-level selection is imposed that requires the presence of at least two charged tracks, of which at least one satisfies all of the criteria listed above. In addition, the total energy deposited in the BSC (E_{sum}) must be greater than $0.28E_{beam}$, and the selected tracks must not all point into the forward ($\cos\theta > 0$) or the backward ($\cos\theta < 0$) hemisphere.

For two-prong events, residual cosmic ray and lepton pair (e^+e^- and $\mu^+\mu^-$) backgrounds are removed by requiring that the tracks not be back-to-back, and that there be at least two isolated energy clusters in the BSC with $E > 100$ MeV that are at least 15° in azimuth from the closest charged track. This last requirement rejects radiative Bhabha events.

These requirements eliminate virtually all cosmic rays and most of the lepton pair (e^+e^- and $\mu^+\mu^-$) events.

The remaining background contributions due to lepton pairs (N_{ll}), including $\tau^+\tau^-$ production above threshold, and two-photon events ($N_{\gamma\gamma}$) are estimated using Monte Carlo simulations and subtracted as indicated in Eq. (1).

Cuts used for selecting hadronic events were varied in a wide range, e.g. $|\cos\theta|$ from 0.75 to 0.90, E_{sum} from $0.24E_{beam}$ to $0.32E_{beam}$ to estimate the systematic error arising from the event selection; this is the dominant component of the systematic error as indicated in Table II.

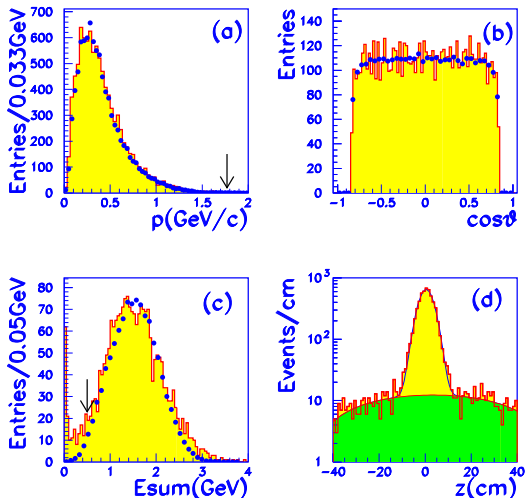


FIG. 1. Distributions for $E_{cm}=3.0$ GeV of (a) track momentum; (b) track $\cos\theta$; (c) total energy deposited in the BSC; and (d) event vertex position along the beam (z) axis. Dots and histograms in (a)-(c) represent Monte Carlo and real data, respectively. The excess at low energy in (c) is due to the beam associated background, which is not simulated in the Monte Carlo.

The numbers of hadronic events and beam-associated background events are determined by fitting the distribution of event vertices along the beam direction with a Gaussian to describe the hadronic events and a polynomial of degree one to three for the beam-associated background. This background varies from 3 to 10% of the selected hadronic event candidates, depending on the energy. The fit using a second degree polynomial, shown in Fig. 1 (d), turned out to be the best. The difference between using a polynomial of degree one or three to that of degree two is about 1%, which is included in the systematic error in the event selection.

The beam-associated background can also be determined by applying the same hadronic event selection criteria to separated-beam data, as described in ref. [6]. The differences between the R values obtained using these two methods range between 0.3 and 2.3%, depending on the energy, and are included in the systematic uncertainty.

The integrated luminosity is determined from the number of large-angle Bhabha events, as described in detail in ref. [6]. The luminosity systematic error includes the uncertainties arising in the selection of the Bhabha events,

the efficiency determination, the background contamination, and the cross section calculation.

A special joint effort was made by the Lund group and the BES collaboration to develop the LUARLW generator, which uses a formalism based on the Lund Model Area Law, but without the extreme-high-energy approximations used in JETSET's string fragmentation algorithm [8]. The final states simulated in LUARLW are exclusive in contrast to JETSET, where they are inclusive. Above 3.77 GeV, the production of D , D^* , D_s , and D_s^* is included in the generator according to the Eichten Model [9]. A Monte Carlo event generator has been developed to handle decays of the resonances in the radiative return processes $e^+e^- \rightarrow \gamma J/\psi$ or $\gamma\psi(2S)$ [10].

The parameters in LUARLW are tuned to reproduce 14 distributions of kinematic variables over the entire energy region covered by the scan [11]. These include the multiplicity, sphericity, angular and momentum distributions, which are shown in Fig. 2. We find that one set of parameter values is required for the cm energy region below open charm threshold, and that a second set is required for higher energies. In an alternative approach, the parameter values were tuned point-by-point throughout the entire energy range. The detection efficiencies determined using individually tuned parameters are consistent with those determined with globally tuned parameters to within 2%. This difference is included in the systematic errors. The detection efficiencies were also determined using JETSET74 for the energies above 3 GeV. The difference between the JETSET74 and LUARLW results is about 1%, and is also taken into account in estimating the systematic uncertainty. Figure 3 (a) shows the variation of the detection efficiency as a function of cm energy.

We changed the branching fractions of D , D^* , D_s , and D_s^* production by 50 % and find that the detection efficiency varies less than 1%. We also varied the fraction of the continuum under the broad resonances by 20 %, and find the change of the detection efficiency is about 1%. These variations are included in the systematic errors.

Different schemes for the initial state radiative corrections were compared [12–15], as reported in ref. [6]. Below charm threshold, the four different schemes agree with each other to within 1%, while above charm threshold, where resonances are important, the agreement is within 1 to 3%. The radiative correction used in this analysis is based on ref. [15], and the differences with the other schemes are included in the systematic error [16].

To calculate δ , a cutoff in s' , the effective cm energy after ISR to produce hadrons, has to be made. In our calculation, the minimum value of s' should be the threshold for producing two pions, corresponding to $x = 1 - s'/s = (0.9805 - 0.9969)$ in the 2-5 GeV range. Our criteria to select hadronic events is such that ϵ approaches zero when x is close to 0.90, which makes us insensitive to events with high ISR photon energy.

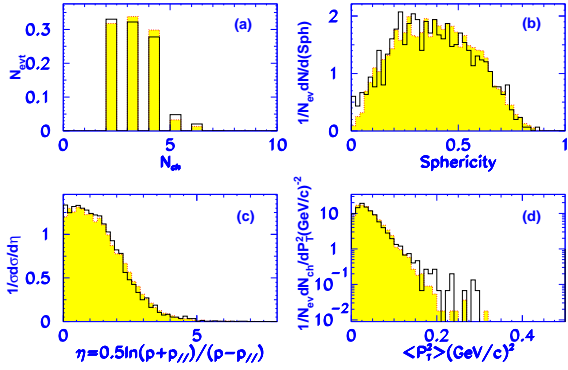


FIG. 2. Comparison of hadronic event shapes at 2.2 GeV between Monte Carlo (shaded region) and data (histogram). (a) Multiplicity, (b) sphericity, (c) rapidity, and (d) transverse momentum.

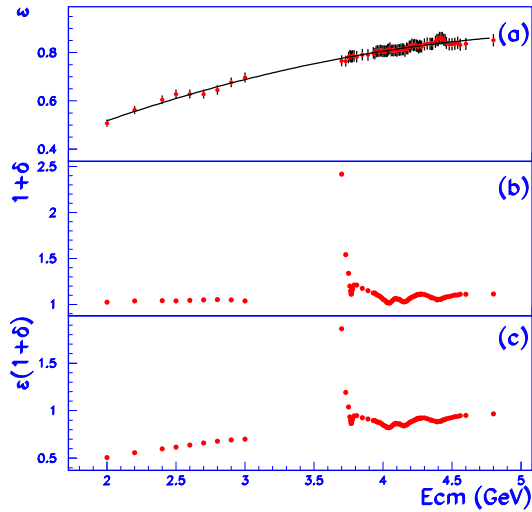


FIG. 3. (a) The cm energy dependence of the detection efficiency for hadronic events estimated using the LUARLW generator. The error bars are the total systematic errors. (b) The calculated radiative correction, and (c) the product of (a) and (b).

In calculating the radiative correction for the narrow resonances J/ψ and $\psi(2S)$, the theoretical cross section is convolved with the energy distribution of the colliding beams, which is treated as a Gaussian with a standard deviation of $1.32 \times 10^{-4} E_{cm}$ (GeV). For the broad resonances at 3770, 4040, 4160, and 4416 MeV, the interferences and the energy-dependence of total widths were taken into consideration. Initially the resonance parameters from PDG2000 [17] were used; then the parameters were allowed to vary and were determined from our fit. The calculation converged after a few iterations.

We varied the input parameters (masses and widths) of the J/ψ , $\psi(2S)$, and the broad resonances used in the radiative correction determination by one standard deviation from the values quoted in ref. [17], and find that the changes in the R value are less than 1% for most points. Points close to the resonance at 4.0 GeV have errors from

1 to 1.7%. Figure 3 (b) shows the radiative correction as a function of cm energy, where the structure at higher energy is related to the radiative tail of the $\psi(2S)$ and the broad resonances in this energy region. Tables I and II list some of the values used in the determination of R and the contributions to the uncertainty in the value of R at a few typical energy points in the scanned energy range, respectively.

TABLE I. Some values used in the determination of R at a few typical energy points.

E_{cm} (GeV)	N_{had}^{obs}	N_{ll+} $N_{\gamma\gamma}$	L (nb $^{-1}$)	ϵ_{had} (%)	$(1 + \delta)$	R	Stat. error	Sys. error
2.000	1155.4	19.5	47.3	49.50	1.024	2.18	0.07	0.18
3.000	2055.4	24.3	135.9	67.55	1.038	2.21	0.05	0.11
4.000	768.7	58.0	48.9	80.34	1.055	3.16	0.14	0.15
4.800	1215.3	92.6	84.4	86.79	1.113	3.66	0.14	0.19

TABLE II. Contributions to systematic errors: hadronic selection, luminosity determination, hadronic efficiency determination, trigger efficiency, radiative corrections and total systematic error. All errors are in percentages (%).

E_{cm} (GeV)	Had. sel.	L	Had. eff.	Trig.	Rad. corr.	tot.
2.000	7.07	2.81	2.62	0.5	1.06	8.13
3.000	3.30	2.30	2.66	0.5	1.32	5.02
4.000	2.64	2.43	2.25	0.5	1.82	4.64
4.800	3.58	1.74	3.05	0.5	1.02	5.14

Table III lists the values of R from this experiment. They are displayed in Fig. 4, together with BESII values from ref. [6] and those measured by MarkI, $\gamma\gamma 2$, and Pluto [2–4]. The R values from BESII have an average uncertainty of about 6.6%, which represents a factor of two to three improvement in precision in the 2 to 5 GeV energy region. Of this error, 4.3 % is common to all points. These improved measurements have a significant impact on the global fit to the electroweak data and the determination of the SM prediction for the mass of the Higgs particle [18]. In addition, they are expected to provide an improvement in the precision of the calculated value of a_{μ}^{SM} [19,20], and test the QCD sum rule down to 2 GeV [21,22].

We would like to thank the staff of the BEPC Accelerator Center and IHEP Computing Center for their efforts. We thank B. Andersson for helping in the development of the LUARLW generator. We also wish to acknowledge useful discussions with M. Davier, B. Pietrzyk, T. Sjöstrand, A. D. Martin and M. L. Swartz. We especially thank M. Tigner for major contributions not only to BES but also to the operation of the BEPC during the R scan.

This work is supported in part by the National Natural Science Foundation of China under Contract Nos. 19991480, 19805009 and 19825116; the Chinese Academy of Sciences under contract Nos. KJ95T-03, and E-

TABLE III. Values of R from this experiment; the first error is statistical, the second systematic.

E_{cm} (GeV)	R	E_{cm} (GeV)	R	E_{cm} (GeV)	R	E_{cm} (GeV)	R
2.000	$2.18 \pm 0.07 \pm 0.18$	3.890	$2.64 \pm 0.11 \pm 0.15$	4.120	$4.11 \pm 0.24 \pm 0.23$	4.340	$3.27 \pm 0.15 \pm 0.18$
2.200	$2.38 \pm 0.07 \pm 0.17$	3.930	$3.18 \pm 0.14 \pm 0.17$	4.130	$3.99 \pm 0.15 \pm 0.17$	4.350	$3.49 \pm 0.14 \pm 0.14$
2.400	$2.38 \pm 0.07 \pm 0.14$	3.940	$2.94 \pm 0.13 \pm 0.19$	4.140	$3.83 \pm 0.15 \pm 0.18$	4.360	$3.47 \pm 0.13 \pm 0.18$
2.500	$2.39 \pm 0.08 \pm 0.15$	3.950	$2.97 \pm 0.13 \pm 0.17$	4.150	$4.21 \pm 0.18 \pm 0.19$	4.380	$3.50 \pm 0.15 \pm 0.17$
2.600	$2.38 \pm 0.06 \pm 0.15$	3.960	$2.79 \pm 0.12 \pm 0.17$	4.160	$4.12 \pm 0.15 \pm 0.16$	4.390	$3.48 \pm 0.16 \pm 0.16$
2.700	$2.30 \pm 0.07 \pm 0.13$	3.970	$3.29 \pm 0.13 \pm 0.13$	4.170	$4.12 \pm 0.15 \pm 0.19$	4.400	$3.91 \pm 0.16 \pm 0.19$
2.800	$2.17 \pm 0.06 \pm 0.14$	3.980	$3.13 \pm 0.14 \pm 0.16$	4.180	$4.18 \pm 0.17 \pm 0.18$	4.410	$3.79 \pm 0.15 \pm 0.20$
2.900	$2.22 \pm 0.07 \pm 0.13$	3.990	$3.06 \pm 0.15 \pm 0.18$	4.190	$4.01 \pm 0.14 \pm 0.14$	4.420	$3.68 \pm 0.14 \pm 0.17$
3.000	$2.21 \pm 0.05 \pm 0.11$	4.000	$3.16 \pm 0.14 \pm 0.15$	4.200	$3.87 \pm 0.16 \pm 0.16$	4.430	$4.02 \pm 0.16 \pm 0.20$
3.700	$2.23 \pm 0.08 \pm 0.08$	4.010	$3.53 \pm 0.16 \pm 0.20$	4.210	$3.20 \pm 0.16 \pm 0.17$	4.440	$3.85 \pm 0.17 \pm 0.17$
3.730	$2.10 \pm 0.08 \pm 0.14$	4.020	$4.43 \pm 0.16 \pm 0.21$	4.220	$3.62 \pm 0.15 \pm 0.20$	4.450	$3.75 \pm 0.15 \pm 0.17$
3.750	$2.47 \pm 0.09 \pm 0.12$	4.027	$4.58 \pm 0.18 \pm 0.21$	4.230	$3.21 \pm 0.13 \pm 0.15$	4.460	$3.66 \pm 0.17 \pm 0.16$
3.760	$2.77 \pm 0.11 \pm 0.13$	4.030	$4.58 \pm 0.20 \pm 0.23$	4.240	$3.24 \pm 0.12 \pm 0.15$	4.480	$3.54 \pm 0.17 \pm 0.18$
3.764	$3.29 \pm 0.27 \pm 0.29$	4.033	$4.32 \pm 0.17 \pm 0.22$	4.245	$2.97 \pm 0.11 \pm 0.14$	4.500	$3.49 \pm 0.14 \pm 0.15$
3.768	$3.80 \pm 0.33 \pm 0.25$	4.040	$4.40 \pm 0.17 \pm 0.19$	4.250	$2.71 \pm 0.12 \pm 0.13$	4.520	$3.25 \pm 0.13 \pm 0.15$
3.770	$3.55 \pm 0.14 \pm 0.19$	4.050	$4.23 \pm 0.17 \pm 0.22$	4.255	$2.88 \pm 0.11 \pm 0.14$	4.540	$3.23 \pm 0.14 \pm 0.18$
3.772	$3.12 \pm 0.24 \pm 0.23$	4.060	$4.65 \pm 0.19 \pm 0.19$	4.260	$2.97 \pm 0.11 \pm 0.14$	4.560	$3.62 \pm 0.13 \pm 0.16$
3.776	$3.26 \pm 0.26 \pm 0.19$	4.070	$4.14 \pm 0.20 \pm 0.19$	4.265	$3.04 \pm 0.13 \pm 0.14$	4.600	$3.31 \pm 0.11 \pm 0.16$
3.780	$3.28 \pm 0.12 \pm 0.12$	4.080	$4.24 \pm 0.21 \pm 0.18$	4.270	$3.26 \pm 0.12 \pm 0.16$	4.800	$3.66 \pm 0.14 \pm 0.19$
3.790	$2.62 \pm 0.11 \pm 0.10$	4.090	$4.06 \pm 0.17 \pm 0.18$	4.280	$3.08 \pm 0.12 \pm 0.15$		
3.810	$2.38 \pm 0.10 \pm 0.12$	4.100	$3.97 \pm 0.16 \pm 0.18$	4.300	$3.11 \pm 0.12 \pm 0.12$		
3.850	$2.47 \pm 0.11 \pm 0.13$	4.110	$3.92 \pm 0.16 \pm 0.19$	4.320	$2.96 \pm 0.12 \pm 0.14$		

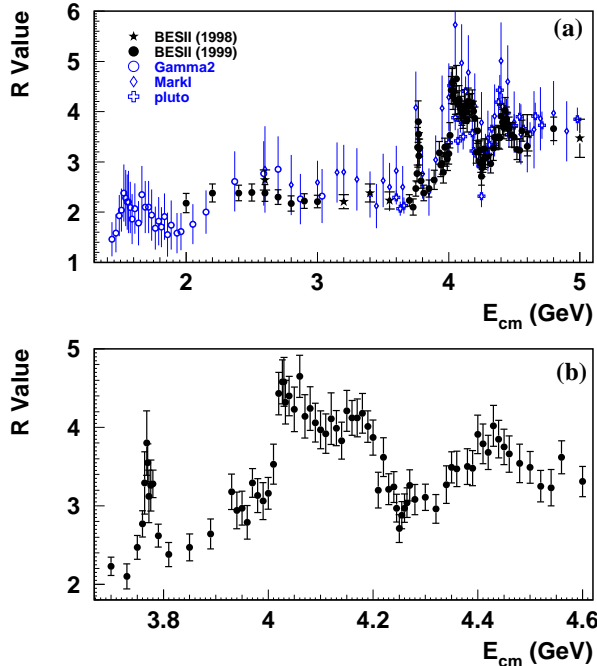


FIG. 4. (a) A compilation of measurements of R in the cm energy range from 1.4 to 5 GeV. (b) R values from this experiment in the resonance region between 3.75 and 4.6 GeV.

01 (IHEP); and by the Department of Energy under Contract Nos. DE-FG03-93ER40788 (Colorado State University), DE-AC03-76SF00515 (SLAC), DE-FG03-

94ER40833 (U Hawaii), DE-FG03-95ER40925 (UT Dallas), and by the Ministry of Science and Technology of Korea under Contract KISTEP I-03-037(Korea).

[1] Z.G. Zhao, International Journal of Modern Physics A15 (2000)3739.
[2] J. L. Siegrist *et al.*, (Mark I Collab.), *Phys. Rev. D* **26**, 969 (1982).
[3] C. Bacci *et al.*, ($\gamma\gamma 2$ Collab.), *Phys. Lett. B* **86**, 234 (1979).
[4] L. Criegee and G. Knies, (Pluto Collab.), *Phys. Rep.* **83**, 151 (1982);
Ch. Berger *et al.*, *Phys. Lett. B* **81**, 410 (1979).
[5] Z.G. Zhao, *Nucl. Phys. A* **675**, 13c (2000).
[6] J. Z. Bai *et al.*, (BES Collab.), *Phys. Rev. Lett.* **84**, 594 (2000).
[7] J.Z. Bai *et al.*, (BES Collab.), *Nucl. Instrum. Methods* **A458**, 627 (2001).
[8] B. Andersson and Haiming Hu, "Few-body States in Lund String Fragmentation Model", hep-ph/9910285.
[9] E. Eichten *et al.*, *Phys. Rev. D* **21**, 203 (1980).
[10] J.C. Chen *et al.*, *Phys. Rev. D* **62**, 034003 (2000).
[11] Haiming Hu *et al.*, "The Application of A New Generator Based on Lund Area Law to the R Scan in 2-5 GeV Center-of-mass Energy Region", Accepted by "High En-

- ergy Physics and Nuclear Physics (China)".
- [12] F.A. Berends and R. Kleiss, *Nucl. Phys. B* **178**, 141 (1981).
 - [13] G. Bonneau and F. Martin, *Nucl. Phys. B* **27**, 387 (1971).
 - [14] E. A. Kuraev and V.S. Fadin, *Sov. J. Nucl. Phys.* **41**, 3(1985).
 - [15] A. Osterheld *et al.*, SLAC-PUB-4160, 1986. (T/E)
 - [16] We extended the calculation of the radiative correction used in ref. 12 to include the contributions of multi-soft photons by means of exponentiation. The results are equivalent to those of ref. 15.
 - [17] Particle Data Group, D.E. Groom *et al.*, *Eur. Phys. J. C* **15**, 1 (2000).
 - [18] H. Burkhardt and B. Pietrzyk, LAPP-EXP 2001-03, accepted by Physics Letters.
 - [19] B. Pietrzyk, Robert Carey, Atul Gurtu, talks given at ICHEP2000, Osaka, Japan, July 2000.
 - [20] A. Martin *et al.*, *Phys. Lett. B* **492**, 69 (2000).
 - [21] M. Davier and A. Hoecker, *Phys. Lett. B* **419**, 419 (1998).
 - [22] J.H. Kuehn and M. Steinhauser, *Phys. Lett. B* **437**, 425 (1998).